

# Reducing parametric backscattering by polarization rotation

Ido Barth<sup>1,\*</sup> and Nathaniel J. Fisch<sup>2</sup>

<sup>1</sup>Princeton Plasma Physics Laboratory, Princeton University, Princeton, New Jersey 08543, USA

<sup>2</sup>Department of Astrophysical Sciences, Princeton University, Princeton, New Jersey 08540, USA

(Dated: December 30, 2018)

When a laser passes through underdense plasmas, Raman and Brillouin Backscattering can reflect a substantial portion of the incident laser energy. This is a major loss mechanism, for example, in inertial confinement fusion. However, by slow rotation of the incident linear polarization, the overall reflectivity can be reduced significantly. Particle in cell simulations show that, for parameters similar to those of indirect drive fusion experiments, polarization rotation reduces the reflectivity by a factor of 5. A general, fluid-model based, analytical estimation for the reflectivity reduction agrees with simulations.

*Introduction.* — Mitigating parametric backscattering (PB) is one of the major challenges in light-matter interaction. For example, in inertial confinement fusion (ICF), PB is responsible for reflecting of about 10% of the total incident lasers energy [1–3]. As a result, less energy is available for the hydrodynamic pellet compression. There are two main types of PB, stimulated Raman backscattering (SRS) and stimulated Brillouin backscattering (SBS). In SRS the incoming energy is backscatter through an electron plasma wave (EPW) while the energy transfer mediator in SBS is an ion acoustic wave. Because of the large ion/electron mass ratio, SRS generally has a higher growth rate than SBS, and therefore generally dominant. In case that SRS is Landau damped (for high electron temperatures) or excluded (for over quarter-critical densities), SBS becomes the dominant scattering mechanism. In the parameter regime relevant to the current design of indirect ICF, SRS is dominant for the inner beams while SBS is dominant for the outer beams [3, 4]. When counter propagating beams cross, PB depends on the relative polarization between the beams [5]. Multibeam SRS, which was recently recognized as a prominent backscattering mechanism, also depends on the polarization arrangement of the crossing beams [6].

Methods to reduce PB in ICF include increasing the electron temperature [2], introducing a thin layer of boroated gold on the inside of the hohlraum wall [2], and a combination of three smoothing methods [7, 8], spatial [9], spectral dispersion [10], and polarization smoothing [11]. Perpendicular polarizations also control the cross beam energy transfer, thereby control symmetry [12]. The complicated scaling of saturation of the plasma waves with temperature was studied experimentally in Ref. [13]. However, although spectral modulations are used for smoothing, the polarization of the beam is always constant.

In this paper, we show that rotation of the polarization of the incident laser can be used to reduce PB. This is because, on the one hand, only the polarization component that is parallel to the incident light polarization is getting amplified (via SBS or SRS), while, on the other hand, light cannot change its polarization when traveling

through a non-magnetized plasma. The combination of these two facts means that slowly rotating or oscillating the incident beam polarization reduces the effective interaction length between the incident laser and a noise component. As a result, the parametric instability noise amplification is depressed, resulting in a reduction in the overall reflectivity. For significant reflectivity reduction, the rotation frequency should be of the order of the parametric growth rate or larger. Although, for rotating polarization, both transverse polarizations contribute the noise amplification, the exponential character of PB results in a reduction of the overall reflectivity. In addition, because the effect is accumulative in the growth rate itself, the reduction becomes more prominent for systems with less initial noise but more e-foldings.

To quantify this effect, we first introduce the rotating polarization light and its effect on PB via one-dimension (1D) particle-in-cell (PIC) simulations and discuss the relevant parameter regimes. Then, we develop a theoretical approach based on the 3-wave interaction fluid model to estimate the reduction in the overall reflectivity and summarize the conclusions.

*Rotating polarization light.* — Consider a vector potential,  $\mathbf{A}$ , of form

$$\mathbf{A}_0 = \Re \left[ a_0 \mathbf{p} e^{i(\omega_0 t - k_0 x)} \right], \quad (1)$$

where,  $\Re$  denotes the real part;  $\mathbf{A}_0$  is in the units of  $m_e c^2/e$ ;  $m_e$  and  $e$  are the electron mass and charge, respectively;  $c$  is the speed of light;  $a_0$  is the (complex) dimensionless amplitude;  $\omega_0$  and  $k_0$  are the laser frequency and wave number, respectively; and  $\mathbf{p}$  is the (time dependent) polarization unit vector,

$$\mathbf{p} = (\hat{y} \cos \Theta + \hat{z} \sin \Theta). \quad (2)$$

Here,  $\hat{y}$ ,  $\hat{z}$  are unit vectors in the transverse direction and  $\Theta = \Theta(t, x)$  is the polarization rotation angle. For simplicity, we consider a simple polarization rotation such that the polarization angle at the plasma boundary is given by  $\Theta(t, x = 0) = \Omega t$ , where  $\Omega$  is the rotating frequency. In other words, in the vacuum (outside the plasma) the polarization angle can be written as  $\Theta = \Omega t'$ ,

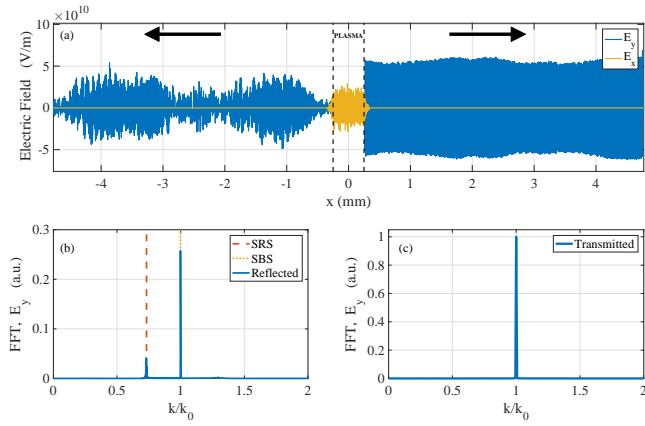


FIG. 1. (color online) Constant polarization. (a) Spatial distribution of the electric fields at the time the incident pulse exit the plasma. (b) Spectral distribution of the reflected ( $x < -0.25$  mm) electromagnetic field,  $E_y$ . (c) Spectral distribution of the transmitted ( $x > 0.25$  mm) electromagnetic field,  $E_y$ .

where  $t' = t - x/c$ . It is important to note that since  $\Omega \neq \omega_0$ , the light polarization is not a circular. Moreover, for  $\Omega \ll \omega_0$  the light can be considered as locally linearly polarized, while its polarization rotates at frequency  $\Omega$ .

Notably, such type of light can be realized by combining two counter-rotating, circularly polarized lasers with frequency difference of  $2\Omega$ ,

$$A_{\pm} = \frac{a_0}{2} [\hat{y} \cos(\omega_{\pm} t') \pm \hat{z} \sin(\omega_{\pm} t')], \quad (3)$$

where  $\omega_{\pm} = \omega_0 \pm \Omega$ . This is because

$$A_+ + A_- = a_0 \cos(\omega_0 t') [\hat{y} \cos(\Omega t') + \hat{z} \sin(\Omega t')] = \mathbf{A}_0. \quad (4)$$

Eqs. (3)-(4) suggest a practical way to create such a rotatingly polarized pulse. First, the incident, linearly polarized, pulse is split into two perpendicular linear polarizations. Second, the beams are frequency shifted, one up and one down. Then, two wave plates are used to convert the beams into right and left circularly polarized. Finally, the two beams,  $A_{\pm}$ , are recombined into a single beam,  $A_0$ , with rotating polarization.

Alternative realizations of such an optical rotation employ, for example, Faraday rotation with time-dependent magnetic field or laser frequency chirp, chirping the pulse frequency and passing through chiral materials, or some combination of these techniques. However the latter techniques might be more challenging because of the short rotation time scale that is required to reduce PB.

*PIC simulations.* — To illustrate the PB reduction effect, we consider parameters similar to those of ICF experiments and compare incident pulse of constant polarization (Fig. 1) with pulse with rotating polarization (Fig. 2). The 1D PIC simulations were run with the code

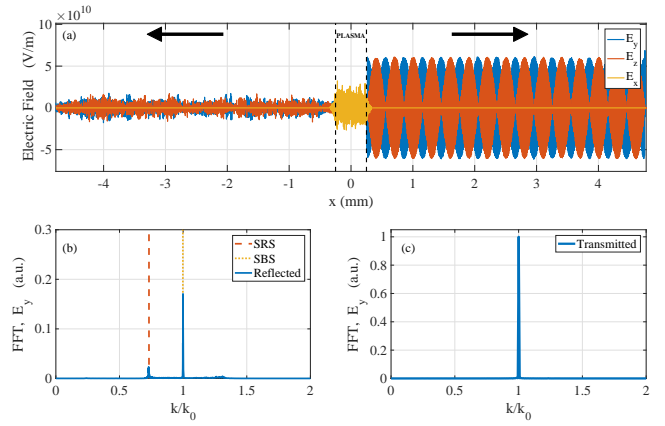


FIG. 2. (color online) Rotating polarization. (a) Spatial distribution of the electric fields at the time the incident pulse exit the plasma. (b) Spectral distribution of the reflected ( $x < -0.25$  mm) electromagnetic field,  $E_y$ . (c) Spectral distribution of the transmitted ( $x > 0.25$  mm) electromagnetic field,  $E_y$ .

EPOCH [14] with 120 cells per  $\mu\text{m}$  and 40 particles per cell. In addition to the physical noise, PIC simulations introduce also numerical noise, which depends on the resolution. Therefore, to preserve the initial background noise, we use the same resolution in all simulations and compared the reduction in the reflectivity.

The physical parameters in the simulations were as follows. The laser wavelength and intensity were  $\lambda_0 = 0.351 \mu\text{m}$  and  $I_0 = 5 \times 10^{14} \text{ W/cm}^2$ ; the pulse duration was  $\tau = 15$  ps; the plasma length and density were  $L = 0.5$  mm and  $n_0 = 5 \times 10^{20} \text{ cm}^{-3}$ ; the electron (ion) temperature was  $T_e = 1000$  eV ( $T_i = 50$  eV). In Fig. 1, we present a non-rotating pulse ( $\Omega = 0$ ) just after passing the plasma. In the figure, the plasma boundaries are depicted by dashed lines and the pulse propagates from left to right. Thus, the left part of Fig. 1a represents the reflected light while the right part is the transmitted pulse. Spectral analysis of the reflected part that is shown in Fig. 1b suggests that the dominant backscattering mechanism in this case is SBS. This is because, in this regime, SRS is Landau damped due to the high electron temperature.

We define the reflectivity

$$R = \frac{U_r}{U_i}, \quad (5)$$

where,  $U_i$  and  $U_r$  are the incident and reflected electromagnetic fluences, respectively. These fluences are calculated by integrating the incident and reflected intensities over time. For example, the reflectivity in the case presented in Fig. 1 is  $R = 0.15$ . Now, we rotate the incident beam with frequency  $\Omega/2\pi = 500\text{GHz}$  and present the electric fields of the two linear polarizations,  $\hat{y}$  and  $\hat{z}$  in Fig. 2a. The overall reflectivity is reduced to the value of  $R = 0.03$ , illustrating the effect of reflectivity reduction.

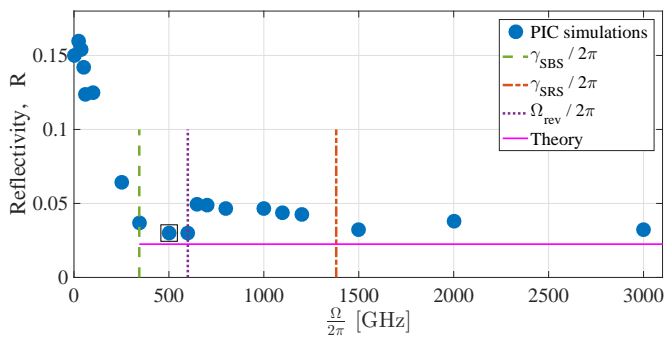


FIG. 3. (color online) Reflectivity versus polarization rotation frequency. The reflectivity reduction occurs at the SBS growth rate (green dashed line) while at the SRS growth rate (red dashed-dotted line),  $R$  is already saturated. Also shown, the theoretical prediction for the reflectivity reduction (magenta solid line) and the revolution frequency (purple dotted line). The black square represents the example of Fig. 2.

We anticipate also a  $\Omega$ -dependency of the reflectivity. For rotation that is too slow, the polarization is effectively fixed for many e-foldings. Therefore, it is clear that in the limit  $\Omega \ll \gamma$ , where  $\gamma$  is the relevant PB growth rate, a negligible reflectivity reduction is predicted. As  $\Omega$  increases and becomes comparable to  $\gamma$ , the polarization rotates within a few e-foldings, effectively reducing the resonant interaction length, thereby reducing also the reflectivity. However, for higher frequencies, say  $\Omega > \gamma$ , the incident laser polarization returns to be parallel to the amplified noise many times within one e-folding and, on average, the effective interaction length is constant. Therefore, no further reduction is then expected, i.e.,  $R$  saturates. This dependency is illustrated in Fig. 3 in which  $R$  is plotted versus  $\Omega$ . It is shown that the reduction begins when  $\Omega \lesssim \gamma$ , reach to a minimum at  $\Omega \approx \gamma$ , and saturates for  $\Omega > \gamma$ . In this regime,  $\gamma$  is the SBS growth rate (because SRS is Landau damped) having the value of  $\gamma = 2.16 \times 10^{12} \text{ sec}^{-1}$ .

Fig. 3 shows another interesting (but smaller) effect in which the saturation of  $R$  for  $\Omega > \gamma$  is not monotonic. The oscillations in  $R$  might be understood by introduction another time scale that may affect the reflectivity. Noting that the passage time of the laser front through the plasma is  $L/c$ , we define the revolution frequency,  $\Omega_{\text{rev}} = 2\pi c/L$  as the rotation frequency in which the polarization performs one revolution when crossing the plasma. Therefore, for  $\Omega = \Omega_{\text{rev}}$  the incident pulse polarization performs a half revolution (e.g., from  $\hat{y}$  to  $-\hat{y}$ ) relative to a point on the counter-propagating backscattered pulse. The phase difference,  $-1 = \exp(i\pi)$  is compensated after a very short time of  $\pi/\omega_0 \approx 0.5\text{fs}$  and the parametric instability returns to be resonant. For the example shown in Fig. 3,  $\Omega_{\text{rev}}/2\pi = 600\text{GHz}$  (dotted purple line), which is when the reflectivity increases from 0.3 to 0.5.

*Theory.* — In order to estimate the reduction in reflectivity,  $R$ , consider one of the polarizations, say  $\hat{y}$ , of the reflecting light,  $\mathbf{A}_1$ , that is amplified from the background noise. The idea is to find the modified linear growth rates and then to compare the amplification of the backscattered intensity with and without rotation. It will be shown that, for rotating polarization, the effective growth rate is smaller, and thus, the total reflectivity is reduced. For simplicity, we assume non relativistic particles and neglect collisional, kinetic, stochastic, and multidimensional effects. However, the comparison with PIC simulations, where all of these effects (except multidimensionality and collisions) are included, provides the physical justification of using this simple model to estimate the reflectivity reduction.

We employ a 1D fluid model to describe the electron (ion) density perturbations,  $n_e$  ( $n_i$ ) normalized by the unperturbed density,  $n_0$ . The Maxwell wave equation describes the reflected light (dimensionless) vector potential,  $\mathbf{A}_1$ , in an unmagnetized plasma while the incident light,  $\mathbf{A}_0$ , is considered constant in the forthcoming linear analysis [15, 16].

$$(\partial_t^2 + \omega_e^2 - c^2 \partial_x^2) \mathbf{A}_1 = -\omega_e^2 n_e \mathbf{A}_0 \quad (6)$$

$$(\partial_t^2 + \omega_e^2 - \gamma_e v_e^2 \partial_x^2) n_e = \omega_e^2 n_i + c^2 \partial_x^2 (\mathbf{A}_0 \cdot \mathbf{A}_1) \quad (7)$$

$$(\partial_t^2 + \omega_i^2 - 3v_i^2 \partial_x^2) n_i = \omega_i^2 n_e. \quad (8)$$

Here,  $\omega_e$  ( $\omega_i$ ) is the electron (ion) plasma frequency;  $n_0$  is the unperturbed average plasma density;  $v_e$  ( $v_i$ ) is the electron (ion) thermal velocity; and  $\gamma_e = 3$  ( $\gamma_e = 1$ ) for adiabatic (isothermal) equation of state associated with EPW (IAW). By using the standard harmonic approximation for the electron and ion density perturbations,

$$n_{e,i} = \Re \left[ \tilde{n}_{e,i} e^{i(\omega t - kx)} \right], \quad (9)$$

and for the vector potential of the reflected light

$$\mathbf{A}_1 = \Re \left[ a_1 \hat{y} e^{i(\omega_1 t + k_1 x)} \right], \quad (10)$$

and by neglecting the interaction terms in the right hand sides of Eqs. (7) and (6), we get the dispersion relations for the two types of longitudinal plasma waves and for the electromagnetic (EM) waves in plasmas

$$\omega^2 = \omega_e^2 + 3v_e^2 k^2 \quad (\text{EPW}) \quad (11)$$

$$\omega = c_s k \quad (\text{IAW}) \quad (12)$$

$$\omega_{0,1}^2 = \omega_e^2 + c^2 k_{0,1}^2 \quad (\text{EM}). \quad (13)$$

For EPW we have neglected the ions motion while for IAW we have assumed  $\omega \ll \omega_e^2$ , neglected the ion thermal velocity,  $v_i$ , and defined  $c_s = \sqrt{T_e/m_i}$ .

Next, we calculate the linear growth rate for rotating polarization incident pulse. Note that because the incident light,  $\mathbf{A}_0$ , in Eq. (1) is (locally) linearly polarized, we considered linear ( $\hat{y}$ ) polarization also for the backscatter

wave in Eq. (10). This polarization is not time dependent though. Therefore, a factor of  $\cos \Theta$  from Eq. (2) will appear in the right hand side of Eqs. (6) and (7). By assuming perfect backward resonance conditions,

$$\omega_1 = \omega_0 - \omega \quad (14)$$

$$k_1 = k - k_0, \quad (15)$$

Eqs. (6)-(8) become

$$(\omega_1^2 - \omega_e^2 - c^2 k_1^2) a_1 = \frac{\omega_e^2}{2} n_e a_0 \cos \Theta \quad (16)$$

$$(\omega^2 - \omega_e^2 - \gamma_e v_e^2 k^2) n_e + \omega_e^2 n_i = -\frac{c^2 k^2}{2} a_0 a_1 \cos \Theta \quad (17)$$

$$(\omega^2 - \omega_i^2 - 3v_i^2 k^2) n_i + \omega_i^2 n_e = 0. \quad (18)$$

By solving Eqs. (16)-(18) for  $\omega$  one finds the linear growth rate,  $\gamma = \text{Im}(\omega)$ . For SRS the ion motion is neglected, i.e.,  $n_i = 0$ , and the growth rate is [15, 16],

$$\gamma = \frac{a_0 c k \sqrt{\omega_e}}{4\sqrt{\omega_b}} |\cos \Theta|, \quad (\text{SRS}) \quad (19)$$

where we neglected thermal corrections and used the EPW (Eq. (11)) and the EM (Eq. (13)) dispersion relations. Similarly, for SBS one finds [15, 16]

$$\gamma = \frac{a_0 c k \omega_i}{4\sqrt{\omega_s \omega_0}} |\cos \Theta|, \quad (\text{SBS}) \quad (20)$$

where  $\omega_s = kc_s$  and the dispersion relations of IAW (Eq. (12)) and EM waves (Eq. (13)) are used.

If the frequency is sufficiently slow, i.e.,  $\Omega \ll \omega_0$ , we can regard  $\gamma$  as a weakly time dependent growth rate. This timescale separation allows us to define an effective e-folding

$$\Gamma = 2 \int_0^{\frac{L}{c}} \gamma dt. \quad (21)$$

The noise intensity is then amplified by a factor of  $e^\Gamma$ . In the limit of constant polarization  $\Theta = 0$ , we get the usual e-folding definition,

$$\Gamma_0 = 2\gamma_0 L/c. \quad (22)$$

Here,  $\gamma_0 = \gamma(\Theta = 0)$  and we assumed that the noise is being amplified through the whole plasma length. In reality, many noise sources throughout the plasma contribute to the reflectivity. Therefore, we replace  $\Gamma_0$  in Eq. (22) by an effective e-folding,  $\bar{\Gamma}_0 < \Gamma_0$ . For homogeneous noise source, this correction can be calculated by defining the average gain,

$$e^{\bar{\Gamma}_0} = \frac{1}{L} \int_0^L e^{2\gamma_0 x/L} dx = \Gamma_0^{-1} (e^{\Gamma_0} - 1). \quad (23)$$

For  $\Gamma_0 > 3$ , this can be simplified into

$$\bar{\Gamma}_0 \approx \Gamma_0 - \ln \Gamma_0. \quad (24)$$

By including the correction of Eq. (24), assuming many polarization rotations in plasma,  $\Omega \gg 2c/L$ , Eq. (21) becomes

$$\Gamma = \frac{2}{\pi} \bar{\Gamma}_0. \quad (25)$$

As a result, the total amplification of the backscatter noise is effectively reduced. In the linear regime, the backscatter intensity can be written as  $I_{\text{reflect}} = I_{\text{noise}} e^\Gamma$ , where  $I_{\text{noise}}$  is the initial (thermal) noise intensity. We note that at a given time and position, only one component of the noise polarization can be amplified, and therefore the total reduction factor is the same as that of the  $\hat{y}$  polarization in Eq. (25). Therefore, the reduced reflectivity can be estimated as

$$R = e^{\Gamma - \bar{\Gamma}_0} R_0 \approx e^{-0.36 \bar{\Gamma}_0} R_0, \quad (26)$$

where,  $R_0$  is the reflectivity of the same incident pulse but without rotating the polarization.

Importantly, Eq. (26) means that the reflectivity reduction factor,  $R/R_0$ , decreases exponentially with  $\Gamma_0$ . In other words, for systems with smaller noise level but with more e-foldings, the reduction effect is more significant. However, since we have linearized the fluid model by neglecting the nonlinear terms in Eqs. (6)-(8), our estimation for the reflectivity reduction, Eq. (26), is valid only in the linear regime,  $R_0 \ll 1$ .

Finally, we estimate the reduction factor for the example presented in Fig. 2. For this case, SRS is Landau damped due to high electron temperature and thus, the relevant PB is SBS. Without rotation, the SBS growth rate for this example is  $\gamma_0 = 2.16 \times 10^{12} \text{sec}^{-1}$  resulting in  $\bar{\Gamma}_0 = 5.2$  e-foldings. Therefore, we estimate the reflectivity reduction as  $R/R_0 = 0.15$ . For reflectivity without rotation (found in PIC simulations),  $R_0 = 0.15$ , the theoretical prediction for the reflectivity in the presence of polarization rotation is  $R = 0.023$ . As shown in Fig. 3 (magenta dotted line) this estimation fairly agrees with the reflectivity obtained in PIC simulations,  $R(\Omega/2\pi = 500\text{GHz}) = 0.03$ , which is associated with reflectivity reduction of  $R/R_0 = 0.2$ .

*Conclusions.* — In summary, we show that by rotating the polarization of an incident light on a plasma, the overall reflectivity can be significantly reduced. For example, PIC simulations show, that for parameters similar to those of an indirect ICF, polarization rotation can reduce the SBS reflectivity by a factor of 5. An analytical estimation, based on the linearized fluid model, agrees with the numerical simulations. In order to get significant reflectivity reduction, the rotation frequency must be of the order of the dominant instability growth rate, but the reduction saturates for higher frequencies. Our theory predicts that the reduction effect is more significant for systems with larger number of e-foldings, provided the system is in linear regime, i.e.,  $R_0 \ll 1$ . Such polarization rotation can be realized by combining two frequency

shifted, counterrotating circularly polarized lasers. Also, different time-dependent modulations (e.g., oscillations) of the incident light polarization are predicted to result in a similar reflectivity reduction. This novel technique might be important for ICF experiments or for other systems where it is essential to reduce backscattering of light passing through a plasma or, for that matter, other dielectric media.

The authors appreciate discussions with P. Michel. This work was supported by NNSA Grant No. de-na0002948, AFOSR Grant No. FA9550-15-1-0391, and DOE Contract No. DE-AC02-09CH11466.

---

\* ibarth@princeton.edu

- [1] R. K. Kirkwood, J. D. Moody, J. Kline, E. Dewald, S. Glenzer, L. Divol, P. Michel, D. Hinkel, R. Berger, E. Williams, J. Milovich, L. Yin, H. Rose, B. MacGowan, O. Landen, M. Rosen, and J. Lindl, *Plasma Phys. Control. Fusion* **55**, 103001 (2013).
- [2] D. E. Hinkel, M. J. Edwards, P. A. Amendt, R. Benedetti, L. Berzak Hopkins, D. Bleuel, T. R. Boehly, D. K. Bradley, J. A. Caggiano, D. A. Callahan, *et al.*, *Plasma Phys. Control. Fusion* **55**, 124015 (2013).
- [3] D. E. Hinkel, M. D. Rosen, E. A. Williams, A. B. Langdon, C. H. Still, D. A. Callahan, J. D. Moody, P. A. Michel, R. P. J. Town, R. A. London and S. H. Langer, *Phys. Plasmas* **18**, 056312 (2011).
- [4] D. E. Hinkel, D. A. Callahan, A. B. Langdon, S. H. Langer, C. H. Still, and E. A. Williams, *Phys. Plasmas* **15**, 056314 (2008).
- [5] R. K. Kirkwood, J. D. Moody, C. Niemann, E. A. Williams, A. B. Langdon, O. L. Landen, L. Divol, L. J. Suter, S. Depierreux, and W. Seka, *Phys. Plasmas* **13**, 082703 (2006).
- [6] P. Michel, L. Divol, E. L. Dewald, J. L. Milovich, M. Hohenberger, O. S. Jones, L. Berzak Hopkins, R. L. Berger, W. L. Kruer, and J. D. Moody, *Phys. Rev. Lett.* **115**, 055003 (2015).
- [7] R. L. Berger, E. Lefebvre, A. B. Langdon, J. E. Rothenberg, C. H. Still, and E. A. Williams, *Phys. Plasmas*, **6**, 1043 (1999).
- [8] J. D. Moody, B. J. MacGowan, J. E. Rothenberg, R. L. Berger, L. Divol, S. H. Glenzer, R. K. Kirkwood, E. A. Williams, and P. E. Young, *Phys. Rev. Lett.* **86**, 2810 (2001).
- [9] S. N. Dixit, J. K. Lawson, K. R. Manes, H. T. Powell, and K. A. Nugent, *Opt. Lett.* **19**, 417 (1994).
- [10] S. Skupsky, R. W. Short, T. Kessler, R. S. Craxton, S. Letzring, and J. M. Soures, *J. Appl. Phys.* {bf 66, 3456 (1989).
- [11] E. Lefebvre, R. L. Berger, A. B. Langdon, B. J. MacGowan, J. E. Rothenberg, and E. A. Williams, *Phys. Plasmas* **5**, 2701 (1998).
- [12] P. Michel, L. Divol, D. Turnbull, and J. D. Moody, *Phys. Rev. Lett.* **113**, 205001 (2014).
- [13] R. K. Kirkwood, R. L. Berger, C. G. R. Geddes, J. D. Moody, B. J. MacGowan, S. H. Glenzer, K. G. Estabrook, C. Decker, and O. L. Landen, *Phys. Plasmas* **10**, 2948 (2003).
- [14] T. D. Arber, K. Bennett, C. S. Brady, A. Lawrence-Douglas, M. G. Ramsay, N. J. Sircombe, P. Gillies, R. G. Evans, H. Schmitz, A. R. Bell, and C. P. Ridgers, *Plasma Phys. Controlled Fusion* **57**, 113001 (2015).
- [15] W. L. Kruer, *The Physics of Laser Plasma Interactions* (Addison-Wesley, Reading, MA, 1988).
- [16] D. W. Forslund, J. M. Kindel, and E. L. Lindman, *Phys. Fluids* **18**, 1002 (1975).